Korean J. Chem. Eng., **27**(3), 939-943 (2010)
DOI: 10.1007/s11814-010-0129-3

Control of oxygen concentration in water using a hollow fiber membrane contactor

Dongjae Jeong, Mihye Yun, Jeongsik Oh, Ina Yum, and Yongtaek Lee†

Department of Chemical Engineering, College of Engineering, Chungnam National University,
220 Gung-dong, Yuseong-gu, Daejeon 305-764, Korea
(*Received 12 May 2009 • accepted 27 September 2009*)

Abstract−A novel theoretical analysis was performed to regulate the oxygen concentration in water using a membrane contactor composed of nonporous hollow fibers. The governing ordinary differential equations were derived for the countercurrent flow of the feed water and the feed gas in a membrane contactor. The governing equations were regarded as a two point boundary value problem. The nonlinear ordinary differential equations were simultaneously solved using a finite difference method. The computer program was coded in Fortran language using the Compaq Visual Fortran Software. It was found that the concentration of oxygen dissolved in water increases from 28.9 to 64.3 ppm as the area of the membrane increases from 1.24 to 3.73 m^2 at the given typical operating condition: the flow rate of the feed gas is kept to be 1.0 L/min; its pressure is maintained to be 4 atm; the flow rate of the water is 15 L/min. It is observed that the concentration of oxygen increases from 48.2 to 56.2 ppm as the concentration of the feed gas increases from 0.75 to 0.95 mole fraction. As the flow rate of the water increases from 15 to 25 L/min, the concentration of oxygen decreases from 56.2 to 38.6 ppm with a constant membrane area of 3.11 m^2.

Key words: Membrane Contactor, Numerical Analysis, Oxygenated Water, Hollow Fiber

INTRODUCTION

A hollow-fiber membrane contactor might be useful for various types of separation, including gas/liquid absorption, liquid/liquid extraction, pervaporation, and degassing of liquids. Recently, the hollow fiber membrane contactor has been effectively applied to control the concentration of the dissolved gases [1-3].

In a membrane contactor, the membrane plays the role of an interface between two phases: gas-liquid or liquid-liquid. Since two phases are separated by a membrane, there are many advantages in operation over the conventional technology in which two phases are to be contacted. First, there is no emulsion droplet. Second, the pressure and the flow rate in each phase are able to be individually controlled. Third, there is neither channeling nor recirculation. Finally, the scale up is relatively easily carried out [4]. The membrane may be either porous or nonporous depending on the application. The membrane contactor has been applied for diverse separation purposes: adsorptive removal of copper ions [5], recovery of Sb(V) [6], purification of gelsolin from plasma [7], separation of the enantiomer with a porous membrane [8] and a hybrid absorber-heat exchanger [9], removal of dissolved O_2 with a nonporous membrane [10]. When a porous membrane is used as an interface, there are two operating modes: the non-wetted mode and the wetted mode. For the non-wetted mode, the membrane pores are filled with a gas since the hydrophobic membrane is normally used. Many researchers have pointed out that the non-wetted operation is preferable during the absorption because the mass transfer coefficient in the non-wetted mode is much bigger than that of the wetted mode [11]. So it can be said that it is always desirable that the absorption process is operated in the non-wetted mode. Karoor and Sirkar comprehensively studied the absorption process of CO_2 and SO_2 in water from mixed gases [12]. If the nonporous membrane is utilized for the gas absorption in a membrane contactor, it is unnecessary to keep the gas pressure always lower than the liquid pressure. In other words, the pressures in the feed side and the permeate side can be separately controlled and the operation of the membrane contactor is much easier and safer than with the porous membrane contactor.

In this study, the absorption of O_2 was theoretically analyzed in a nonporous membrane contactor that was designed to be operated in a countercurrent flow mode. The nonlinear ordinary differential equations were developed and solved using a personal computer. Several operating variables were considered to find their effects on the concentration of O_2 dissolved in water: the O_2 concentration in a feed gas, the flow rate of water, the pressure of a feed gas and the area of a membrane contactor.

NUMERICAL ANALYSIS

1. System Governing Equations

The ordinary differential equations are derived in order to describe O_2 absorption into a liquid flowing through the hollow fiber membrane.

Several assumptions were taken into account when the equations were developed. The gas flows as a plug flow through the shell side. The water also flows as a plug flow through the lumen side. Since the water is usually fed as a turbulent flow, the velocity profile seems to be almost flat along the radius. Therefore, the water flow can be reasonably assumed to be a plug flow for the purpose modeling the system. To simplify the system, it was assumed in both the gas flow and the water flow that there is no mixing along the longitudinal direction. However, there is a perfect mixing across the radial direc-

†To whom correspondence should be addressed.
E-mail: ytlee@cnu.ac.kr

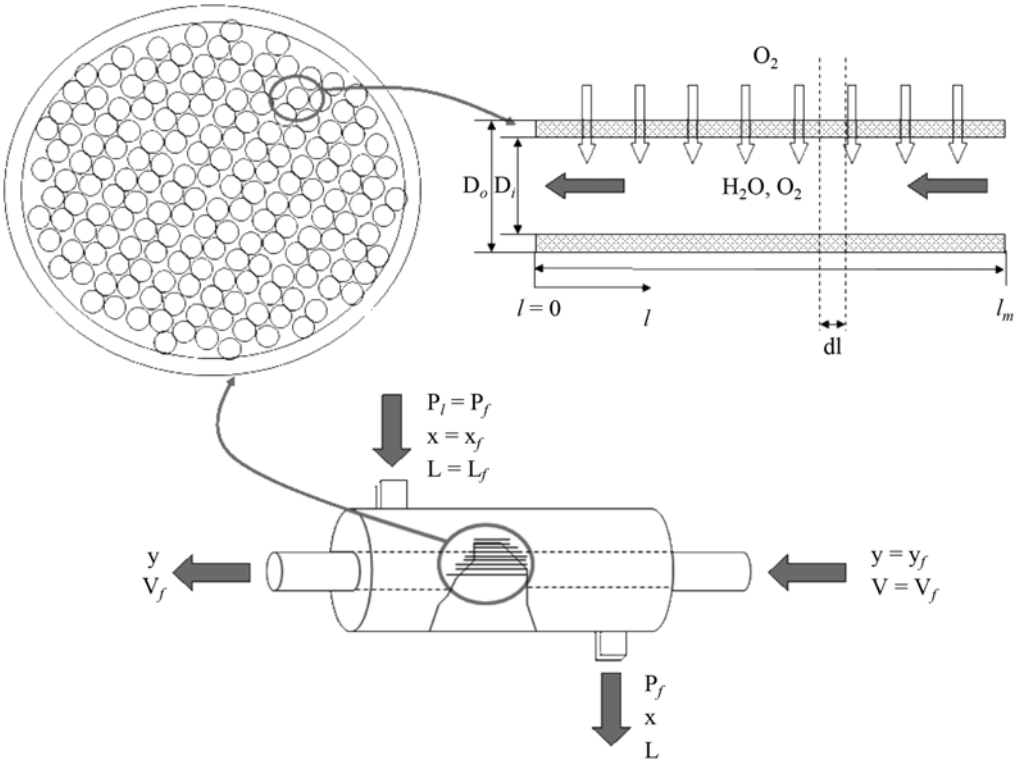

Fig. 1. A schematic of countercurrent flow in hollow fiber membrane contactor.

tion for the water flow so that the O_2 permeate through the membrane wall is well mixed together with the present O_2 in water, leading to the new homogeneous O_2 concentration. The pressures of the gas and the water are kept constant.

Fig. 1 shows a schematic of countercurrent flow in a hollow fiber membrane contactor. The ordinary differential equations can be derived by combining the total mass balance and the mass balance of O_2 in a finite membrane length of dl. x and y represent the mole fraction of O_2 in the feed gas and in the liquid, respectively. L and V are the flow rate of the feed gas and the liquid, respectively. P_1 is the pressures of the feed gas. D_i and D_o are the inside and the outside diameters of the membrane. l denotes the length from the inlet point of the liquid and l_m represents the total length of the membrane.

The total mass balance of a membrane module for a countercurrent flow is represented by

$$L_f = L - V_f(y - y_f) \tag{1}$$

where L_f and V_f are the molar flow rates of a feed gas and a liquid, respectively.

Total mass balance of O_2 is described as

$$L_f \cdot x_f - V_f \cdot y_f = L \cdot x - V_f \cdot y \tag{2}$$

where x_f represents the mole fraction of O_2 in the feed gas at the entrance.

The differential mass balance of O_2 in a finite membrane length of dl can be described as follows:

$$d(V_f \cdot y) = -\pi \cdot \overline{D_{LM}} \cdot dl \cdot \left(\frac{Q}{d}\right)_{O_2} \cdot (P_1 \cdot x - p_2^*) \tag{3}$$

where $(Q/d)_{O_2}$ represents the permeance of oxygen through the membrane. $\overline{D_{LM}}$ represents the logarithmic mean diameter of a hollow fiber membrane. p_2^* denotes a partial pressure corresponding to the molar concentration of oxygen dissolved in water. p_2^* can be obtained using Henry's Law. In other words, Henry's law is applied to calculate the equivalent partial vapor pressure of O_2 in water, which is corresponding to the concentration of O_2 dissolved in water as in Eq. (4)

$$p_2^* = H_{O_2} \cdot y \tag{4}$$

After substituting Eq. (4) into Eq. (3) and dividing each term by dl, rearranging results in the following Eq. (5):

$$\frac{d(V_f \cdot y)}{dl} = -\pi \cdot \overline{D_{LM}} \cdot \left(\frac{Q}{d}\right)_{O_2} \cdot (P_1 \cdot x - H_{O_2} \cdot y) \tag{5}$$

For the constant V_f, Eq. (5) can be reduced to

$$V_f \cdot \frac{dy}{dl} = -\pi \cdot \overline{D_{LM}} \cdot \left(\frac{Q}{d}\right)_{O_2} \cdot (P_1 \cdot x - H_{O_2} \cdot y) \tag{6}$$

The variation of the mole fraction of oxygen dissolved in water along the length of the membrane fiber is as follows:

$$\frac{dy}{dl} = -\frac{1}{V_f} \cdot \pi \cdot \overline{D_{LM}} \cdot \left(\frac{Q}{d}\right)_{O_2} \cdot (P_1 \cdot x - H_{O_2} \cdot y) \tag{7}$$

Differentiating Eq. (1) by dl gives as follows:

Left hand side: $\frac{L_f}{dl} = 0$

Right hand side: $\frac{dL}{dl} - \frac{d(V_f \cdot y)}{dl} + \frac{d(V_f \cdot y_f)}{dl}$

By rearranging the left hand side and the right hand side, the following equation can be obtained:

$$\frac{dL}{dl} = V_f \frac{dy}{dl} \tag{8}$$

Substituting Eq. (7) into Eq. (8) results in

$$\frac{dL}{dl} = -\pi \cdot \overline{D_{LM}} \cdot \left(\frac{Q}{d}\right)_{O_2} \cdot (P_1 \cdot x - H_{O_2} \cdot y) \tag{9}$$

Differentiating Eq. (2) by dl gives as follows:

$$\text{Left hand side: } \frac{d(L_f \cdot x_f)}{dl} - \frac{d(V_f \cdot y_f)}{dl} = 0$$

$$\text{Right hand side: } L \cdot \frac{dx}{dl} + x \cdot \frac{dL}{dl} - V_f \frac{d(y)}{dl}$$

Rearranging the left hand side and the right hand side, the following equation can be obtained:

$$\frac{dx}{dl} = -\frac{1}{L}\left(x \cdot \frac{dL}{dl} - V_f \cdot \frac{dy}{dl}\right) \tag{10}$$

Substituting Eq. (8) into Eq. (10) gives

$$\frac{dx}{dl} = -\frac{1}{L}\left[x \cdot \left(V_f \cdot \frac{dy}{dl}\right) - V_f \cdot \frac{dy}{dl}\right] = -\frac{1}{L}\left[(x-1) \cdot V_f \cdot \frac{dy}{dl}\right] \tag{11}$$

By substituting Eq. (7) into Eq. (11), the variation of oxygen concentration in the feed gas along the fiber length is as follows:

$$\frac{dx}{dl} = -(1-x) \cdot \frac{1}{L}\left[\pi \cdot \overline{D_{LM}} \cdot \left(\frac{Q}{d}\right)_{O_2} \cdot (P_1 \cdot x - H_{O_2} \cdot y)\right] \tag{12}$$

Eqs. (12), (7) and (9) were rearranged to be dimensionless:

$$dx/dl^* = -K_1(\gamma_1 x - \gamma_2 y)(1-x)/L^* \tag{13}$$

$$dy/dl^* = -K_1(\gamma_1 x - \gamma_2 y) \tag{14}$$

$$dL^*/dl^* = -K_1(\gamma_1 x - \gamma_2 y) \tag{15}$$

where l^* represents the normalized length from the inlet point of the liquid. L^* denotes the normalized flow rate of the gas.

The minus sign in the right hand side of Eq. (13) indicates that the mole fraction of O_2 in the feed gas decreases as l^* increases. From Eq. (14), the mole fraction of O_2 in water is expected to increase as l^* increases. The flow rate of the gas will decrease proportionally to the difference of the partial vapor pressures of O_2 between the gas phase and the liquid phase. There are several parameters that appear in Eqs. (13)-(15) and they are defined as follows:

$$\gamma_1 \equiv P_1/P_f \tag{16}$$

$$\gamma_2 \equiv H_{O_2}/P_f \tag{17}$$

$$l^* \equiv l/l_m \tag{18}$$

$$L^* \equiv L/V_f \tag{19}$$

$$K_1 \equiv \pi \cdot \overline{D_{LM}} \cdot l_m \cdot (Q/d)_{O_2} \cdot P_f/V_f \tag{20}$$

The boundary conditions are given by:

$$\text{at } l^*=0,\ x=x_f,\ P_1=P_f,\ L=L_f \tag{21}$$

$$\text{at } l^*=1,\ V=V_f,\ y=y_f \tag{22}$$

Since the boundary conditions are given at two end points, these differential equations are subject to the two point boundary value problem.

2. Calculations

Table 1 represents the basic characteristics of the nonporous hollow fiber membrane used for the computer simulation. Fig. 2 shows the flow diagram of the Fortran program.

Table 1. Characteristic of the hollow fiber membrane contactor

Permeance of oxygen ($mol \cdot Pa^{-1} \cdot m^{-2} \cdot sec^{-1}$)	1.1662×10^{-10}
Hollow fiber O.D. (m)	4×10^{-4}
Hollow fiber I.D. (m)	2.2×10^{-4}
Number of hollow fibers (ea)	9,000
Effective thickness (m)	0.1×10^{-6}

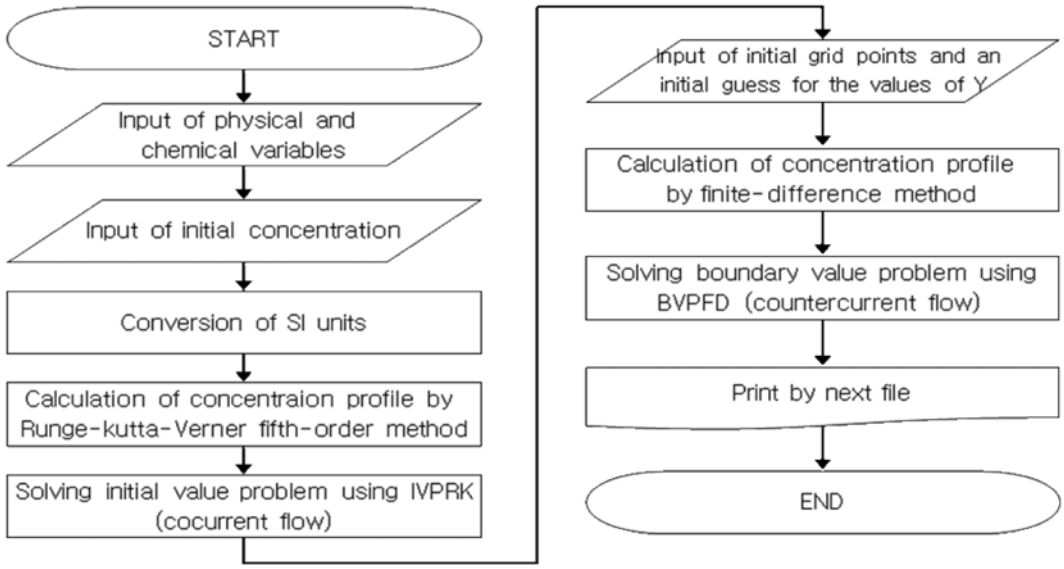

Fig. 2. Flow diagram of Fortran program.

Table 2. Operating conditions for numerical analysis

Flow rate of gas (L/min)	1.0
Flow rate of water (L/min)	15-25
Concentration of oxygen in feed gas (mole fraction)	0.795-0.995
Concentration of oxygen in feed water (ppm)	8
Pressure of feed gas (atm)	2-4
Length of membrane (m)	0.2-0.6
Temperature of water (K)	298.15

A Fortran program for absorption of O_2 was developed using the Compaq Visual Fortran 6.6 software. The system governing equations were thought to be a boundary-value problem and the nonlinear ordinary differential equations were simultaneously solved using the Runge-Kutta-Verner method. The coupled nonlinear differential equation could be simultaneously solved using Compaq Visual Fortran where several subroutines were utilized: IMSL Math/Library. A numerical analysis was carried out with the typical operating conditions as shown in Table 2.

RESULTS AND DISCUSSION

Fig. 3 shows the typical dimensionless profiles versus the dimensionless distance in a membrane contactor with a countercurrent flow pattern. The concentration of O_2 in water increases from 8 ppm to 56.25 ppm as the normalized length of the membrane increases from 0 to 1.

Fig. 4 shows the O_2 concentration in water as a function of the area of the membrane with three different liquid flow rates. The O_2 concentration in water is found to increase as the area increases. Since the contact time of water flowing along the membrane increases as the membrane area increases, it results in the increase of O_2 concentration in water. As the liquid flow rate decreases, the O_2 concentration increases due to the same reason as the area of the membrane.

Fig. 5 shows the outlet O_2 concentration in water versus the O_2 concentration in a feed gas with a parameter of the flow rate of the

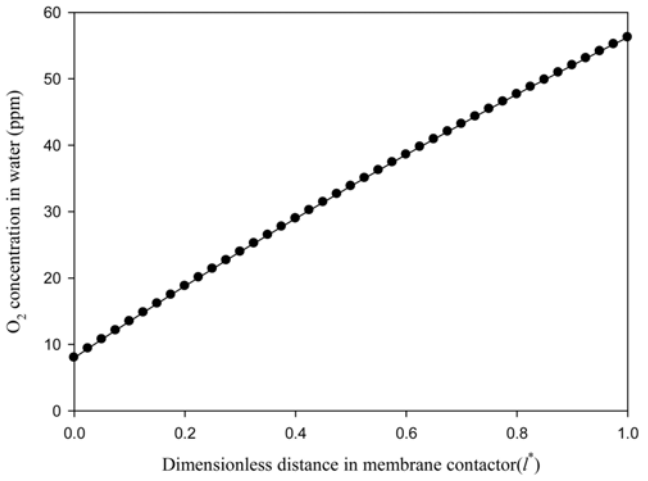

Fig. 3. Typical concentration profile of O_2 in water at different position in membrane contactor (L_f=1.0 L/min, x_f=0.995, L= 0.5 m, P_f=4 atm).

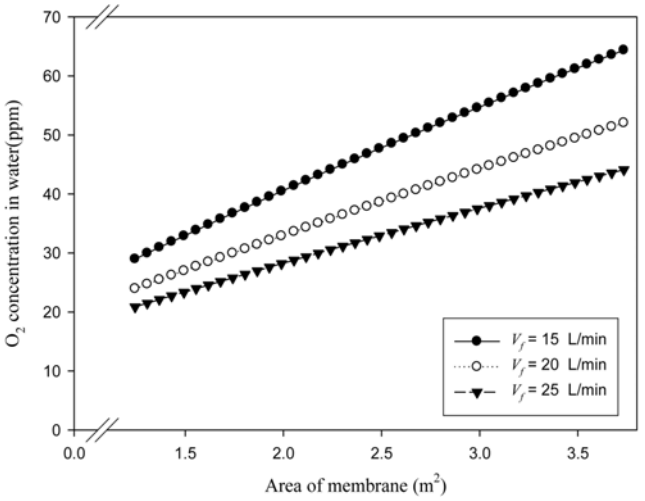

Fig. 4. Concentration of O_2 in water at outlet vs. area of membrane (L_f=1.0 L/min, x_f=0.995, P_f=4 atm).

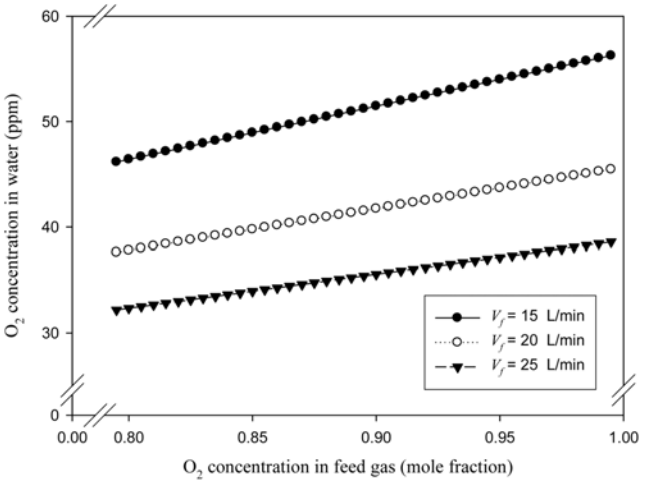

Fig. 5. Concentration of O_2 in water at outlet vs. concentration of O_2 in feed gas (L_f=1.0 L/min, L=0.5 m, P_f=4 atm).

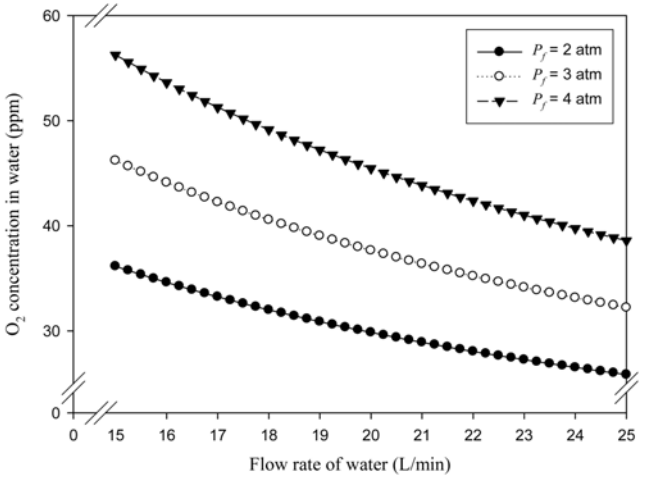

Fig. 6. Concentration of O_2 in water at outlet vs. flow rate of water (L_f=1.0 L/min, x_f=0.995, Area=3.11 m^2).

feed liquid. If the flow rate of water increases, the contact time of water with the membrane gets shorter, leading to the lower O_2 concentration in the outlet water. As the O_2 concentration in a feed gas increases, the driving force increases. Then the O_2 flux increases, resulting in the increase of the O_2 concentration in water.

Fig. 6 shows the outlet O_2 concentration in water versus the flow rate of the feed water with 3 different gas pressure. As expected, the outlet O_2 concentration increases as the pressure of the feed gas increases since the driving force increases. In the meantime, as the flow rate of the water increases, the O_2 concentration decreases since the contact time decreases.

CONCLUSIONS

A novel set of coupled nonlinear ordinary differential equations were developed so that the concentration of oxygen dissolved in water was theoretically analyzed. The numerical computer simulation on the O_2 absorption could be carried out using the Compaq Visual Fortran software, where the coupled nonlinear ordinary differential equations were converted to the coded computer program. The absorption of O_2 from the feed gas could be successfully explored as functions of various parameters. At a higher concentration of O_2 in a feed gas, smaller flow rate of water, higher pressure of the feed gas and larger area of the membrane, a higher absorption of O_2 in water can be observed. It can be said that the operation parameters can be designed to control the concentration of oxygen dissolved in water by a membrane contactor.

ACKNOWLEDGMENTS

This research was supported by ITEP of the Ministry of Commerce, Industry and Energy (Project No. 10026573-2006-01) and partially by Brain Korea 21 Project of Innovative Graduate School of Energy and Environmental Materials in Daedeok Innopolis, Chungnam National University.

NOMENCLATURE

$\overline{D_{LM}}$: log mean diameter of hollow fiber [m]
D_i : inside diameter of hollow fiber [m]
D_o : outside diameter of hollow fiber [m]
K_1 : dimensionless parameter as defined in Eq. (20)
L : flow rate of gas stream [$L \cdot min^{-1}$]
L_f : flow rate of feed gas stream [$L \cdot min^{-1}$]
L^* : dimensionless parameter as defined in Eq. (19)
l : length from the inlet point of the liquid [m]
l_m : total length of the hollow fiber [m]
l^* : normalized length from the inlet point of the liquid as defined in Eq. (18)
P_f : pressure of feed gas stream [atm]
P_1 : pressure of gas stream [atm]
$(Q/d)_{O_2}$: permeance of oxygen gas [$mol \cdot m^{-2} \cdot s^{-1} \cdot kPa^{-1}$]
R : gas constant [$m^3 \cdot Pa \cdot mol^{-1} \cdot K^{-1}$]
T : temperature [K]
V_f : flow rate of water [$L \cdot min^{-1}$]
x : oxygen concentration in gas stream [mole fraction]
x_f : oxygen concentration in feed gas stream [mole fraction]
y : oxygen concentration in feed liquid stream [mole fraction]
y_f : oxygen concentration in feed liquid stream [mole fraction]

Greek Letters

γ_1 : dimensionless pressure ratio as defined in Eq. (16)
γ_2 : dimensionless pressure ratio as defined in Eq. (17)

REFERENCES

1. P. S. Kumar, J. A. Hogendoorn, P. H. M. Feron and G. F. Versteeg, *J. Membr. Sci*., **213**, 231 (2003).
2. M. Mavroudi, S. P. Kaldis and G. P. Sakellaropoulos, *Fuel*, **82**, 2153 (2003).
3. G. B. Kim, S. J. Kim, C. U. Hong, T. K. Kwon and N. G. Kim, *Korean J. Chem. Eng*., **22**, 521 (2005).
4. Y. S. Kim and S. M. Yang, *Sep. Purif. Technol*., **21**, 101 (2000).
5. C. Liu and R. Bai, *J. Membr. Sci*., **284**, 313 (2006).
6. H. Kawakita, K. Uezu, S. Tsuneda, K. Saito, M. Tamada and T. Sugo, *Hydrometallurgy*, **81**, 190 (2006).
7. K. Hagiwara, S. Yonedu, K. Saito, T. Shiraishi, T. Sugo, T. Tojyo and E. Katayama, *J. Chromatogr. B*, **821**, 153 (2005).
8. P. Hadik, L. Kotsis, M. Enisznè-Bódogh, L. Szabó and E. Nagy, *Sep. Purif. Technol*., **41**, 299 (2005).
9. J. Chen, H. Chang and S. R. Chen, *Int. J. Refrigeration*, **29**, 1043 (2006).
10. A. Ito, K. Yamagiwa, M. Tamura and M. Furusawa, *J. Membr. Sci*., **145**, 111 (1998).
11. H. Kreulen, C. A. Smolders, G. F. Versteeg and W. P. M. Van Swaaij, *Chem. Eng. Sci*., **48**, 2093 (1993).
12. S. Karoor and K. K. Sirkar, *Ind. Eng. Chem. Res*., **32**, 674 (1993).